Proc. 6th International Conference on Civil Engineering
Isfahan, Iran, May 5-7 2003
Keynote Lecture

Hydraulic Engineering into the 21st Century: a Rediscovery of the Wheel ? (2) New Challenges

Hubert CHANSON, Reader, h.chanson@mailbox.uq.edu.au
Dept of Civil Engineering, The University of Queensland, Brisbane QLD 4072, Australia

Abstract
Hydraulics has been at the forefront of science for centuries. In this paper, new exciting developments are presented in terms of energy dissipation and multiphase flows. These include the hydraulic design of rectangular dropshafts and stepped chutes for embankment dams, and new air-water studies of spillway flows and dam break waves. The findings demonstrate innovative hydraulic research which must be supported by active and sustained funding.
Keywords: *hydraulic engineering, challenges, energy dissipation, air entrainment, dropshaft, stepped chute, dam break wave, metrology*

1- Introduction

Hydraulic engineers have had an important role to contribute to our Society although the technical challenges are gigantic, often involving interactions between water, solids, air and biological life. The extreme complexity of hydraulic engineering is closely linked with the geometric scale of water systems, the variability of river flows and the complexity of basic fluid mechanics with governing equations characterised by non-linearity and natural fluid instabilities. Although the end of the 20th century marked a change of perception in our society, with more focus on environmental sustainability and management, new exciting developments in hydraulic engineering are presented: i.e., the design of energy dissipators and air-water flow measurements.

2. Energy Dissipation

2.1 Introduction

In hydraulic structures, flood waters must be carried safely above, beside or below. Whether the waters rush as open channel flow, free-falling jet, or pipe flow, it is essential to dissipate a major part of the flow kinetic energy to avoid damage to the channel, the surroundings and to the structure itself. Energy dissipation is usually achieved by a high velocity water jet taking off from a flip bucket and impinging into a downstream plunge pool acting as a water cushion, a standard stilling basin at the chute downstream end where a hydraulic jump is created to dissipate a large amount of flow energy, a dropshaft structure, or the construction of steps on the chute to assist in energy dissipation (Fig. 2-1 & 2-3). In the three first methods, most energy dissipation takes place at the downstream end in the plunge pool, in the stilling basin and in the shaft respectively. At a stepped spillway, the steps increase significantly the rate of energy dissipation taking place in the

chute, and eliminate or reduce the need for a large downstream energy dissipator.

In this section, new developments in energy dissipation structures are presented. First the design of rectangular dropshafts with applications to sewers, culvert and storm water systems. Second the hydraulics of embankment stepped spillways operating with skimming flows.

Fig. 2-1 : Rectangular dropshaft in operation (shaft dimensions: 0.76 m × 0.75 m)
(A) Regime R1 (B) Regime R3

2.2 Dropshaft design

A dropshaft is an energy dissipator connecting two channels with different invert elevations (Fig. 2-1). Ancient dropshafts were built by the Romans. Some aqueducts were equipped with series (or cascades) of dropshafts in Western Europe and North Africa predominantly (CHANSON 2002a). Although dropshaft structures are commonly used in modern sewers and storm water systems, the hydraulics and air-water flow properties of dropshafts have not been systematically documented (APELT 1984, RAJARATNAM et al. 1997). A full-scale study was conducted in the rectangular dropshaft shown in Figure 2-1 (CHANSON 2002b). The drop in invert was 1.7 m, the shaft pool was 1.0 m deep. The inflow and outflow channels were 0.5 m wide and 0.30 m deep. The results provide new insights on dropshaft operation.

The upstream and downstream channels operated as free-surface flows. Three flow regimes were observed as functions of the flow rate. At low flow rates, the free-falling nappe impacted into the shaft pool (regime R1, Fig. 2-1A). For intermediate discharges, the free-falling nappe impacted into the outflow channel (regime R2). Little air bubble entrainment was observed in the pool and very-large invert pressure fluctuations were observed. At large flow rates, the free-jet impacted onto the opposite wall above the downstream conduit obvert (regime R3, Fig. 2-1B).

Detailed air-water flow measurements were conducted with a sturdy single-tip conductivity in the flow regimes R1 and R3. Typical distributions of centreline void fraction C are presented in Figure 2-2, where x is the horizontal distance measured from the downstream shaft wall, and z is the vertical direction positive downwards with z = 0 at the pool free-surface. Experimental results demonstrated high void fractions close to

the free-surface ($z/d_c < 2$) for all flow conditions (Fig. 2-2). In regime R1, the plunging jet flow was characterised by smooth, derivative profiles of void fractions (Fig. 2-2). The centreline data illustrated consistently the advective diffusion of entrained air associated with a quasi-exponential decay of maximum air content with longitudinal distance from impingement and a broadening of the air diffusion layer. The data were best fitted by an analytical solution of the diffusion equation for air bubbles :

Fig. 2-2 : Air concentration distributions beneath the pool free-surface on the shaft centreline ($d_c/h = 0.017$, Regime R1) - Comparison with Equation (2-1)

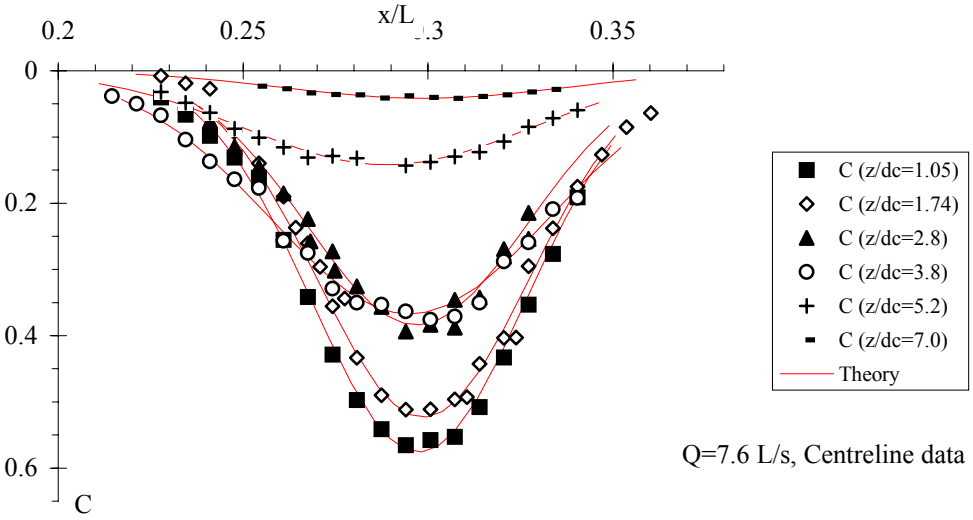

Table 2-1 : *Statistical properties of bubble chord size distributions (centreline data) in a rectangular dropshaft (CHANSON 2002b)*

Q	z	x	Nb of bubbles	Air chord			
				Mean	Std	Skew	Kurt
m^3/s	mm	mm		mm	mm	(Fisher)	(Fisher)
(1)	(2)	(3)	(4)	(5)	(6)	(7)	(8)
0.0076	30	215-240	7650	28.2	54.5	3.6	16.7
(regime R1)	50	216-241	10500	20.8	39.4	3.7	19.0
	80	216-241	7650	15.2	29.0	4.2	23.6
	110	207-232	10157	13.3	24.8	5.2	49.8
	150	207-232	7896	11.9	21.8	6.1	68.5
	200	207-232	3014	10.7	16.2	3.8	21.8
0.067	30	16-31	8199	25.4	44.0	3.6	18.9
(regime R3)	50	16-31	9456	16.5	28.4	3.6	17.4
	150	04-19	10165	7.7	12.8	4.4	23.7
	250	04-19	6855	7.9	15.9	5.4	45.0
	350	10-25	6074	10.2	17.4	5.3	41.9

$$C = \frac{1}{2} * \frac{\frac{Q_{air}}{Q}}{\sqrt{8 * \pi * D^{\#} * \frac{z}{d_i}}} * \left(\exp\left(- \frac{\left(\frac{x - x_i}{d_i} - \frac{1}{2} \right)^2}{2 * D^{\#} * \frac{z}{d_i}} \right) + \exp\left(- \frac{\left(\frac{x - x_i}{d_i} + \frac{1}{2} \right)^2}{2 * D^{\#} * \frac{z}{d_i}} \right) \right) \quad (2\text{-}1)$$

where Q_{air} is the volume air flow rate, d_i is the thickness of the free-jet at impact and x_i is the jet impact coordinate, and $D^{\#}$ is a dimensionless air bubble diffusivity (CHANSON 1997). Equation (2-1) is shown in Figure 2-2, where the values of $D^{\#}$ and Q_{air}/Q were

determined from the best fit of the data.

Bubble chord length distributions were measured. Statistical properties of chord size distributions are summarised in Table 2-1. The results highlighted mean bubble sizes between 10 and 20 mm typically. For all flow conditions, the data demonstrated the broad spectrum of bubble chord lengths from less than 0.5 mm to more than 25 mm. The chord length distributions were skewed with a preponderance of small bubble sizes relative to the mean. The probability of bubble chord length was the largest for bubble sizes between 0 and 2 mm although the mean chord size was much larger (Table 2-1). The trends were emphasised by positive skewness and large kurtosis (Table 2-1, columns 7 and 8). Overall the results were consistent with experimental measurements in the developing flow region of vertical plunging jets (CUMMINGS and CHANSON 1997, CHANSON et al. 2002), although the prototype dropshaft measurements showed larger entrained bubble sizes.

Fig. 2-3 : Melton dam secondary spillway on 30 January 2000 - Completed in 1916, the Melton dam was equipped in 1994 with a secondary spillway (Q_{des} = 2,800 m^3/s, h = 0.6 m)

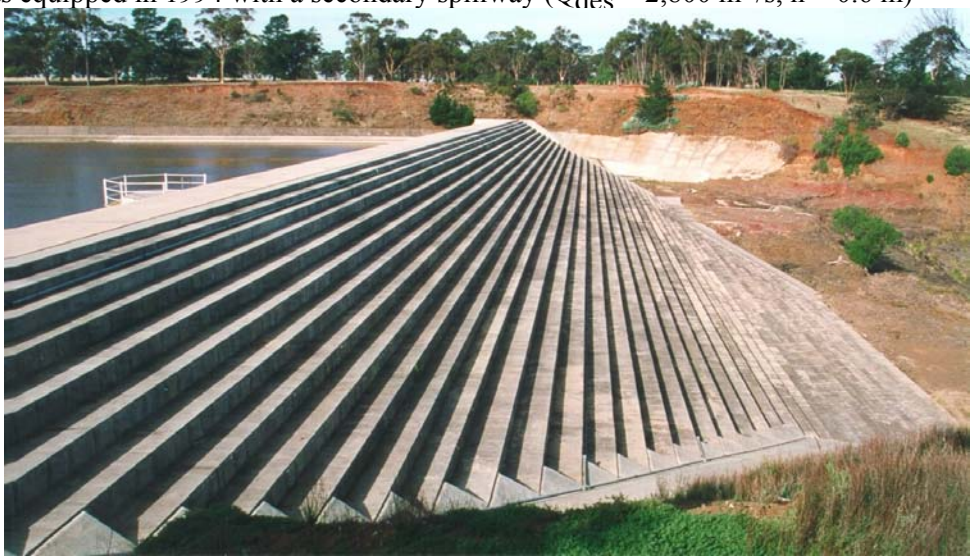

2.3 Skimming flow down embankment stepped spillways

Stepped chutes have been used for more than 3,500 years (CHANSON 2001). At the end of the 19th century, the stepped spillway design accounted for nearly one third of all spillway constructions in North-America. The design technique was abandoned in the late 1920s with new progresses in the energy dissipation characteristics of hydraulic jumps. In the last four decades, the regain of interest for stepped spillways has been associated with the development of new construction techniques (e.g. roller compacted concrete) and new design techniques (e.g. embankment overtopping protection systems, Fig. 2-3). During the 1990s, the construction of secondary stepped spillways accounted for nearly two thirds of dam construction in USA (DITCHEY and CAMPBELL 2000). While most research on stepped spillway hydraulics focused on steep chutes for gravity dams ($\theta \sim 50^o$), recent studies brought new insights into the complicated hydrodynamics of embankment chute overflows.

Visual observations highlighted strong interactions between free-surface and turbulent flow. At the upstream end, the flow was non-aerated but free-surface instabilities were observed (CHANSON and TOOMBES 2002a,2002c). Strong air-water mixing was observed downstream of the inception point of free-surface aeration. Detailed air-water flow measurements demonstrated large amounts of entrained air. Typical experimental data are shown in Figure 2-4 for one flow rate down a 16º stepped chute.

The results illustrate longitudinal oscillations of flow properties. These were observed on steep and flat slopes (e.g. MATOS 2000, CHANSON and TOOMBES 2002c). It is believed that this seesaw pattern and longitudinal undulations result from strong interference between free-surface and vortex shedding behind each step edge.

In skimming flows, cavity recirculation and fluid exchange between cavities and main stream are very energetic and contribute to form drag. Energy considerations provide a relationship between cavity ejection frequency, form drag and energy dissipation. At uniform equilibrium, the head loss between adjacent step edges equals the step height, while energy is dissipated in the cavity at a rate proportional to the ejection frequency F_{ej}, the volume of ejected fluid and the main flow velocity V. It yields:

$$\frac{F_{ej} * (h*\cos\theta)}{V} \approx \frac{f}{5} \qquad (2\text{-}2)$$

where f is the Darcy-Weisbach friction factor, h is the step height and θ is the chute slope (CHANSON et al. 2002b).

Observed longitudinal oscillations of depth-averaged flow properties affect in turn flow resistance calculations. For example, in Figure 2-4, the friction slope calculated between adjacent steps would range between +0.1 to +0.4 for an average value of S_f = 0.20. Professionals should be very critical of spurious claims by some hydraulician on an "unique" flow resistance estimate. CHANSON et al. (2002b) presented a comprehensive re-analysis of more than 700 model and prototype stepped chute data. They compared the results with an analytical solution of the form drag generated by the step cavity flows. Their analysis yielded f ~ 0.2.

Fig. 2-4 : Longitudinal distributions of mean air contents C_{mean}, dimensionless air-water depth Y_{90}/d_c, clear-water depth d/d_c, air-water velocity V_{90}/V_c and mean flow velocity U_w/V_c - Stepped chute: θ = 16°, h = 0.05 m, d_c/h = 1.7 - Measurements conducted at step edges

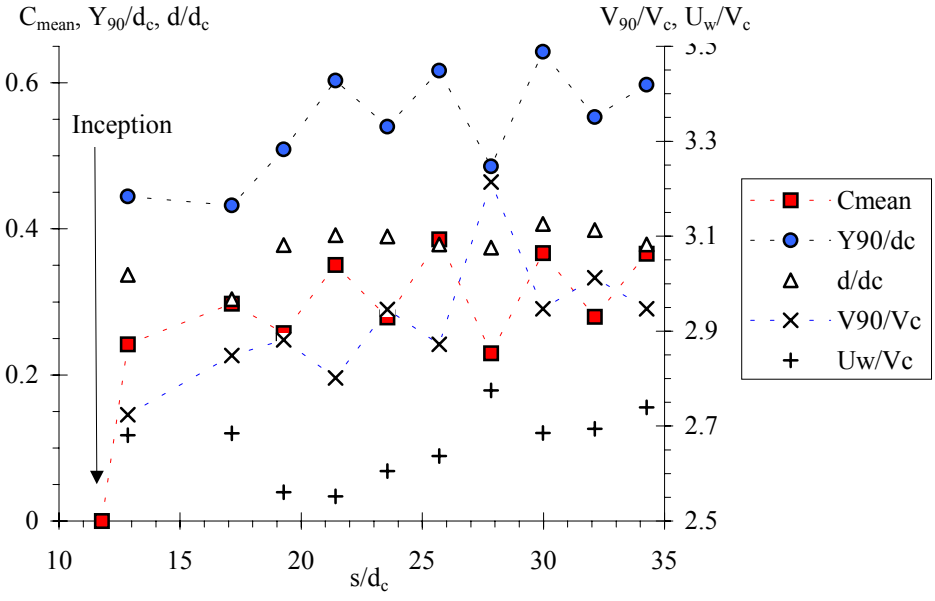

3. Air-water flows in water engineering and hydraulic structures

3.1 Presentation

In Nature, air-water flows are commonly encountered at waterfalls, in mountain torrents and at wave breaking. 'White waters' are also observed in aesthetical fountains and in hydraulic structures (e.g. PLUMPTRE 1993, CHANSON 1997). One of the first scientific accounts was made by LEONARDO DA VINCI (AD 1452-1519) (Fig. 3-1). He

described air-water flow situations, calling the air-water mixture foam (*schiuma*) and white waters (*bianchezza*) (CHANSON 1997 pp. 327-329). LEONARDO DA VINCI recognised with discernment that air entrainment is related to the flow velocity.

Air-water flows have been studied recently compared to classical fluid mechanics. The first successful experimental investigations were conducted by hydraulic engineers during the mid-20th century. That is, EHRENBERGER (1926) in Austria, and STRAUB and ANDERSON (1958) in North-America. Since, the contribution of hydraulic engineers to gas-liquid flow research has been modest. Fundamental research has been dominated by chemical, mechanical and nuclear engineers. For example, the intrusive phase-detection needle probe design was developed by Professor S.G. BANKOFF (NEAL and BANKOFF 1963,1965); phase detection optical fibre probes were developed in the late 1960s (JONES and DELHAYE 1976) despite dubious claims by hydraulicians! In 2003, hydraulic professionals and researchers lack advanced multiphase flow expertise. In the following paragraphs, new developments in air-water flows are presented: turbulence and interface measurements in self-aerated flows, and unsteady air-water flow measurements.

Fig. 3-1 : Sketch of plunging jet flow at a pipe outlet by LEONARDO DA VINCI - Original drawing from about AD 1509 possibly called "sketch of waterfall" or "impact of water on water"

3.2 Air-water flow measurements in self-aerated flows

In hydraulic engineering, classical measurement devices (e.g. Pitot tube, LDV) are affected by entrained bubbles and might lead to inaccurate readings. When the void fraction C exceeds 10 to 15%, and when the liquid fraction (1-C) is larger than 5 to 10%, the most robust instrumentation is the intrusive phase detection probes : optical fibre probe and conductivity/resistivity probe (JONES and DELHAYE 1976, BACHALO 1994, CHANSON 1997,2002c). The intrusive probe is designed to pierce bubbles and droplets (Fig. 3-2A). A typical probe signal output is shown in Figure 3-2B. Although the signal is theoretically rectangular, the probe response is not exactly square because of the finite size of the tip, the wetting/drying time of the interface covering the tip and the response time of the probe and electronics.

The basic probe outputs are the void fraction, bubble count rate and bubble chord time distributions with both single-tip and double-tip probe designs. The void fraction C is the proportion of time that the probe tip is in the air. The bubble count rate F is the number of bubbles impacting the probe tip. The bubble chord times provide information on the air-water flow structure. For one-dimensional flows, chord sizes distributions may be derived (e.g. CHANSON et al. 2002).

Fig. 3-2 : Local air-water flow measurements in skimming flow down a stepped chute (θ = 16º, h = 0.05 m, d_c/h = 1.7) with a double-tip conductivity probe (scan rate: 20 kHz per tip, ∅ = 0.025 mm, Δx = 7.8 mm) - C = 0.08, V = 2.3 m/s, F = 118 Hz, y = 7 mm, step 17

(A) Sketch of bubble impact on phase-detection probe tips (dual-tip probe design)

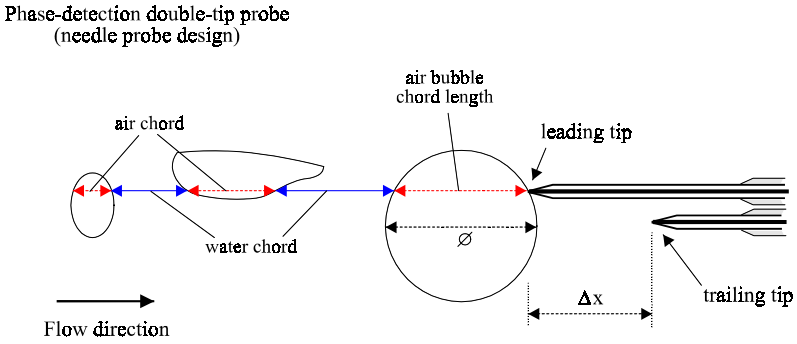

(B) Voltage outputs from a double-tip conductivity probe

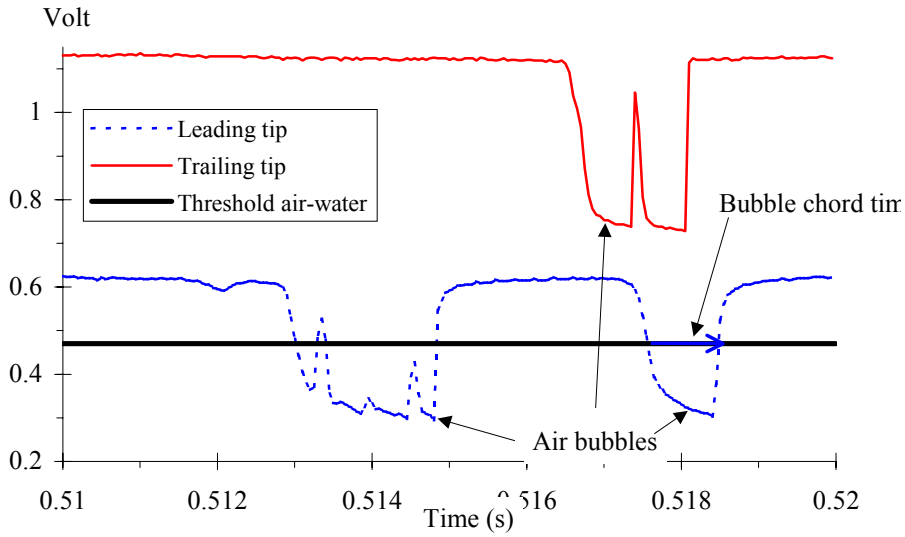

(C) Normalised auto-correlation and cross-correlation functions

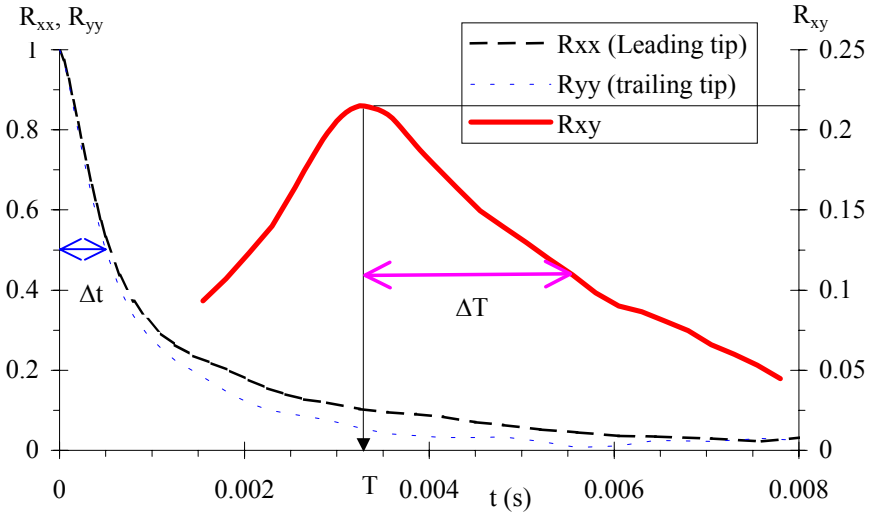

A dual-tip probe design (Fig. 3-2A) provides additionally the air-water velocity, specific interface area, chord length size distributions and turbulence level. The velocity

measurement is based upon the successive detection of air-water interfaces. In turbulent air-water flows, it is common to use a cross-correlation technique (CROWE et al. 1998) and the time-averaged air-water velocity equals :

$$V = \frac{\Delta x}{T} \quad (3\text{-}1)$$

where Δx is the distance between tips and T is the time for which the cross-correlation function is maximum (Fig. 3-2C). The shape of the cross-correlation function provides further information on the velocity fluctuations (App. I). The turbulent intensity may be derived from the broadening of the cross-correlation function compared to the auto-correlation function :

$$Tu = \frac{u'}{V} = 0.851 * \frac{\sqrt{\Delta T^2 - \Delta t^2}}{T} \quad (3\text{-}2)$$

where ΔT as a time scale satisfying : $R_{XY}(T+\Delta T) = R_{XY}(T)/2$, R_{XY} is the normalised cross-correlation function, and Δt is the characteristic time for which the autocorrelation function R_{XX} equals 0.5 (App. I). The autocorrelation function itself provides some information on the air-water flow structure. A dimensionless integral length scale is:

$$I_L = 0.851 * \frac{\Delta t}{T} \quad (3\text{-}3)$$

Chord sizes may be calculated from raw probe signal outputs. The results provide a complete characterisation of the streamwise distribution of air and water chords (e.g. CHANSON and TOOMBES 2002a). The measurement of air-water interface area is a function of void fraction, velocity, and bubble sizes. For any bubble shape, bubble size distribution and chord length distribution, the specific air-water interface area a may be derived from continuity :

$$a = \frac{4 * F}{V} \quad (3\text{-}4)$$

where a is defined as the air-water interface area per unit volume of air and water and Equation (3-4) is valid in bubbly flows ($C < 0.3$). In high air content regions, the flow structure is more complex and the specific interface area a becomes simply proportional to the number of air-water interfaces per unit length of flow ($a \propto 2*F/V$).

3.3 Air-water flow measurements in dam break waves

Air-water flow measurements in unsteady flows are rare, although prototype observations of sudden spillway releases and flash floods highlighted strong aeration of the leading edge of the wave associated with chaotic flow motion (Fig. 3-3). Figure 3-3 shows a dam break wave propagation down a stepped waterway: the wave propagated as a succession of free-falling nappes (Fig. 3-3A) and horizontal runoff downstream of nappe impact (Fig. 3-3B).

Unsteady air-water flow experiments were recently performed in a 25 m long stepped flume with a flat stepped invert (Table 3-1). A sudden flow rate was released down the initially-dry stepped chute, and air-water flow properties were measured with an array of single-tip conductivity probes located on the channel centreline (Fig. 3-3B). The processing technique was adapted for unsteady flow conditions (CHANSON 2003a). Local void fractions were calculated over a time $\tau = \Delta X/C_S$ where C_S is the measured surge front celerity and ΔX is the control volume streamwise length. Measurements were conducted for three flow rates and two steps at distances X' = 0.2, 0.4, 0.6, 0.8 and 1.0 m where X' is measured from the vertical step edge. The main results are outlined below. Typical results are presented in Figure 3-4.

Figure 3-4 shows dimensionless distributions of void fractions at one location X' =

1.0 m for several times ($t-t_s$) and ΔX = 70, 210 and 385 mm, where t_s is the time of passage of wave front. The legend indicates the control volume streamwise length ΔX and dimensionless time $(t-t_s)*\sqrt{g/d_o}$, where d_o is a measure of the initial flow rate Q(t=0+):

$$d_o = \frac{9}{4} * \sqrt[3]{\frac{Q(t=0+)^2}{g * W^2}} \quad (3\text{-}5)$$

and W is the channel width. For an ideal dam break, d_o would be equivalent to the initial water depth behind the dam. The data are compared with corresponding steady flow data (CHANSON and TOOMBES 2002b). The distributions of void fractions demonstrated a very strong aeration of the leading edge for $(t - t_s)*\sqrt{g/d_o} < 1.1$. In Figure 3-4, the data for $(t - t_s)*\sqrt{g/d_o}$ = 0.25, 0.46, 0.66 and 2.11 yielded depth-average void fractions defined between 0 and 90% of C_{mean} = 0.47, 0.54, 0.40 and 0.25 respectively. In steady flow, the mean air content was C_{mean} = 0.20. At the front of the wave, the void fraction distributions had roughly a linear shape :

$$C = 0.90 * \frac{y}{Y_{90}} \qquad (t - t_s)*\sqrt{g/d_o} < 1.2 \quad (3\text{-}6)$$

Fig. 3-3 : Leading edges of dam break wave flows - Advancing flood waves down a stepped chute (3.4º slope, h = 0.07 m, W = 0.5 m) (High-speed photographs)
Right : Step 10, Q(t=0+) = 0.065 m^3/s, free-falling nappe at brink of step 10 plunging onto step 11 - Left : 3.4º slope, Q(t=0+) = 0.055 m^3/s, h = 0.07 m, looking upstream at advancing wave on step 16, with a series of conductivity probes in foreground

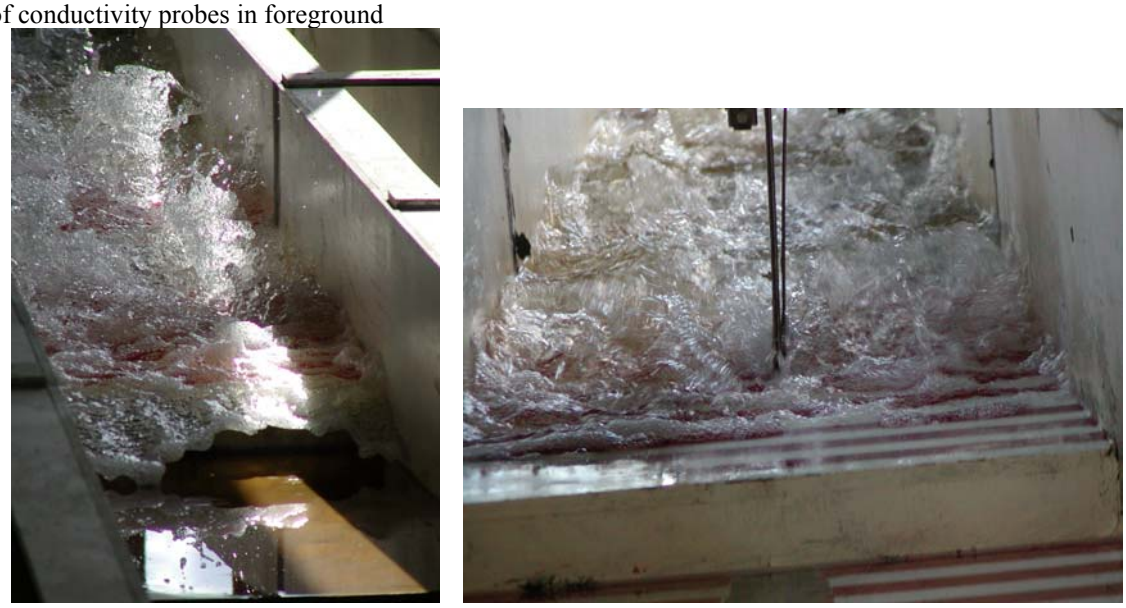

Table 3-1 - *Summary of air-water flow measurements in dam break wave flows*

Reference	θ (deg.)	h m	Q(t=0+) (m^3/s)	Air-water flow measurements	Remarks
(1)	(2)	(3)	(4)	(5)	(6)
CHANSON	3.4	0.071			18 horizontal steps (l = 1.2 m, W = 0.5 m).
(2003a)			0.040	Step 16	
			0.055	Step 16	
			0.075	Steps 10 & 16	

Notes : h : step height; l : step length; Q(t=0+) : initial flow rate; W : chute width.

Fig. 3-4 : Dimensionless void fraction distributions behind the wave front leading edge (Q(t=0+) = 0.075 m^3/s, h = 0.07 m, Step 10, C_S = 2.61 m/s, X' = 10 m) - Comparison with steady flow data (CHANSON and TOOMBES 2002b), and Equations (3-6) and (3-7)

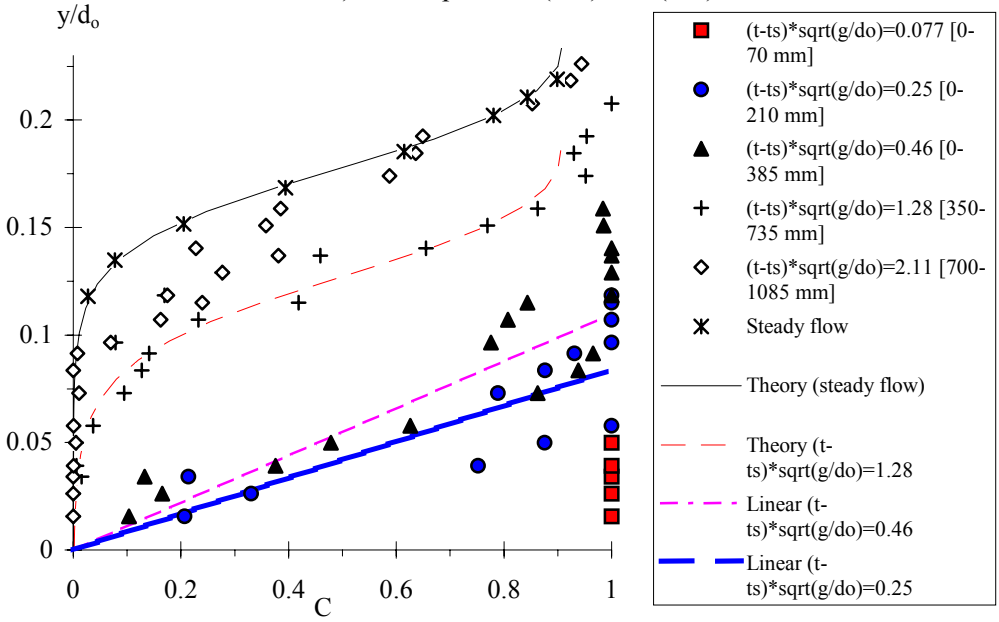

where Y_{90} is the location where C = 90%. Equation (3-6) is a limiting case of the analytical solution of air bubble diffusion equation for steady transition flows down stepped chute (CHANSON and TOOMBES 2002a). For larger times $(t-t_S)$, the distribution of air concentration may be described by a advective diffusion model:

$$C = 1 - \tanh^2\left(K' - \frac{\frac{y}{Y_{90}}}{2 * D_o} + \frac{\left(\frac{y}{Y_{90}} - \frac{1}{3}\right)^3}{3 * D_o}\right) \qquad (t - t_S)*\sqrt{g/d_o} > 1.3 \quad (3\text{-}7)$$

where K' and D_o are functions of the mean air content only (CHANSON and TOOMBES 2002a). Equations (3-6) and (3-7) are plotted for steady and unsteady flow conditions in Figure 3-4. For all experiments, a major change in void fraction distribution shape took place for $(t-t_S)*\sqrt{g/d_o} \sim 1.2$ to 1.5. Possible explanations may include non hydrostatic pressure distributions at the leading wave front, some change in air-water flow structure associated with a change in rheological fluid properties, a change in gas-liquid flow regime, with a plug/slug flow regime in front a homogenous bubbly flow region behind, and some alteration in shear stress distributions and boundary friction.

Bubble and water chord times were measured in dam break wave flows. The bubble chord time t_{ch} was defined as the time spent by the bubble on the probe tip. Results were expressed in terms of pseudo-chord length ch defined as $ch = C_S * t_{ch}$ where C_S is the wave front celerity (CHANSON 2003a). For all flow rates and step locations, the data demonstrated a broad range of bubble chord lengths from less than 0.5 mm to larger than 15 mm. The bubble chord size distributions were skewed with a preponderance of small bubble sizes relative to the mean. The results emphasised the complicated structure of the air-water flow.

4. Summary and Conclusion

Hydraulic engineers were scientific leaders for centuries. Famous applications include the qanats and the first air-water flow experiments by EHRENBERGER.

Although the complexity of hydraulic problems linking air, soil and water is considerable, the writer has shown new innovative developments in hydraulic engineering ranging from basic structures to more advanced topics including air entrainment in dam break wave. These exciting developments demonstrate innovative hydraulic engineering which must be associated with active research and dynamic teaching (CHANSON 2003b). The writer believes that scholarship and quality expertise are the future of hydraulic engineering into the 21st century. He hopes that this lecture will enlighten students, academics and engineers on the future of hydraulics for the benefits of our Society.

5. Acknowledgments

The writer acknowledges the assistance of past and present students, including Dr L. TOOMBES, MM. Carlos GONZALEZ, Chung-hwee Jerry LIM, Craig RUSSELL, York-wee TAN and Joel WILSON.

6. Appendix I : Velocity measurements with dual-tip probes

With phase-detection intrusive probes, velocity measurement is based upon the successive detection of bubbles/droplets by two sensors (Fig. 3-2). In highly turbulent gas-liquid flows, the successive detection of a bubble by each probe tip is highly improbable, and it is common to use a cross-correlation technique. The shape of the cross-correlation function provides a further information on the turbulent velocity fluctuations. Flat cross-correlation functions are associated with large velocity fluctuations around the mean. Thin high cross-correlation curves are characteristics of small turbulent velocity fluctuations. The information must be corrected to account for the intrinsic noise of the leading probe signal. The dimensionless turbulent velocity fluctuations Tu may be estimated from the broadening of cross-correlation function compared to auto-correlation function :

$$Tu = \frac{u'}{V} = \frac{\sqrt{\sigma_{xy}^2 - \sigma_{xx}^2}}{T} \quad (I\text{-}1)$$

where u' is the root mean square of longitudinal component of turbulent velocity, V is the local time-averaged air-water velocity, σ_{xy} is the standard deviation of the cross-correlation function, and σ_{xx} is the standard deviation of the autocorrelation function. Equation (I-1) is based upon an extension of the mean value theorem for definite integrals. Experimental results in turbulent air-water flows demonstrated that both cross-correlation and auto-correlation functions followed a Gaussian distribution (e.g. Fig. 3-2C). Assuming that the successive detections of bubbles by the probe sensors is a true random process, Equation (I-1) yields :

$$\frac{u'}{V} = 0.851 * \frac{\sqrt{\Delta T^2 - \Delta t^2}}{T} \quad (I\text{-}2)$$

where ΔT as a time scale satisfying : $R_{xy}(T+\Delta T) = 0.5\ R_{xy}(T)$, R_{xy} is the normalised cross-correlation function, Δt is the characteristic time for which the normalised autocorrelation function R_{xx} equals 0.5. CHANSON and TOOMBES (2002a) gave a comprehensive explanation of the development.

7. References

APELT, C.J. (1984). "Goonyella Railway Duplication Drop Structures and Energy Dissipators at Culvert Outlets. Model Studies." *Report CH27/84*, Dept. of Civil Engineering, University of Queensland, Australia, Feb., 10 pages, 11 figures & 37 plates.

BACHALO, W.D. (1994). "Experimental methods in Multiphase Flows." *Intl Jl of Multiphase Flow*, Vol. 20, Suppl., pp. 261-295.

CHANSON, H. (1997). "Air Bubble Entrainment in Free-Surface Turbulent Shear Flows." *Academic Press*, London, UK, 401 pages.

CHANSON, H. (2001). "The Hydraulics of Stepped Chutes and Spillways." *Balkema*, Lisse, The Netherlands, 418 pages.

CHANSON, H. (2002a). "An Experimental Study of Roman Dropshaft Hydraulics." *Jl of Hyd.*

Res., IAHR, Vol. 40, No. 1, pp. 3-12.
CHANSON, H,. (2002b). "An Experimental Study of Roman Dropshaft Operation : Hydraulics, Two-Phase Flow, Acoustics." *Report CH50/02*, Dept of Civil Eng., Univ. of Queensland, Brisbane, Australia.
CHANSON, H. (2002c). "Air-Water Flow Measurements with Intrusive Phase-Detection Probes. Can we Improve their Interpretation ?." *Jl of Hyd. Engrg.*, ASCE, Vol. 128, pp. 252-255.
CHANSON, H. (2003a). "Sudden Flood Release down a Stepped Cascade." *Report CH51/03*, Dept of Civil Eng., Univ. of Queensland, Brisbane, Australia.
CHANSON, H. (2003b). "Hydraulic Engineering into the 21st Century: the Rediscovery of the Wheel ? (1) A Review." *Proc. 6th Intl Conf. on Civil Eng.*, Isfahan, Iran, May 5-7, Keynote lecture, 1st part, 12 pages.
CHANSON, H., AOKI, S., and HOQUE, A. (2002). "Similitude of Air Bubble Entrainment and Dispersion in Vertical Circular Plunging Jet Flows. An Experimental Study with Freshwater, Salty Freshwater and Seawater." *Coastal/Ocean Engineering Report*, No. COE02-1, Dept. of Architecture and Civil Eng., Toyohashi University of Technology, Japan, 94 pages.
CHANSON, H., YASUDA, Y., and OHTSU, I. (2002b). "Flow Resistance in Skimming Flows and its Modelling." *Can Jl of Civ. Eng.*, Vol. 29, No. 6, pp. 809-819.
CHANSON, H., and TOOMBES, L. (2002a). "Air-Water Flows down Stepped chutes : Turbulence and Flow Structure Observations." *Intl J of Multiphase Flow*, Vol. 27, 1737-1761.
CHANSON, H., and TOOMBES, L. (2002b). "Energy Dissipation and Air Entrainment in a Stepped Storm Waterway: an Experimental Study." *Jl of Irrigation and Drainage Engrg.*, ASCE, Vol. 128, No. 5, pp. 305-315.
CHANSON, H., and TOOMBES, L. (2002c). "Experimental Investigations of Air Entrainment in Transition and Skimming Flows down a Stepped Chute." *Can. Jl of Civil Eng.*, Vol. 29, No. 1, pp. 145-156.
CROWE, C., SOMMERFIELD, M., and TSUJI, Y. (1998). "Multiphase Flows with Droplets and Particles." *CRC Press*, Boca Raton, USA, 471 pages.
CUMMINGS, P.D., and CHANSON, H. (1997). "Air Entrainment in the Developing Flow Region of Plunging Jets. Part 2 : Experimental." *Jl of Fluids Eng.*, Trans. ASME, Vol. 119, No. 3, pp. 603-608.
DITCHEY, E.J., and CAMPBELL, D.B. (2000). "Roller Compacted Concrete and Stepped Spillways." *Intl Workshop on Hydraulics of Stepped Spillways*, Zürich, Switzerland, Balkema Publ., pp. 171-178.
EHRENBERGER, R. (1926). "Wasserbewegung in steilen Rinnen (Susstennen) mit besonderer Berucksichtigung der Selbstbelüftung." ('Flow of Water in Steep Chutes with Special Reference to Self-aeration.') *Zeitschrift des Österreichischer Ingenieur und Architektverein*, No. 15/16 and 17/18 (in German) (translated by Wilsey, E.F., U.S. Bureau of Reclamation).
JONES, O.C., and DELHAYE, J.M. (1976). "Transient and Statistical Measurement Techniques for two-Phase Flows : a Critical Review." *Intl Jl of Multiphase Flow*, Vol. 3, pp. 89-116.
MATOS, J. (2000). "Hydraulic Design of Stepped Spillways over RCC Dams." *Intl Workshop on Hydraulics of Stepped Spillways*, Zürich, Switzerland, Balkema Publ., pp. 187-194.
NEAL, L.S., and BANKOFF, S.G. (1963). "A High Resolution Resistivity Probe for Determination of Local Void Properties in Gas-Liquid Flows." *Am. Inst. Chem. Jl*, Vol. 9, pp. 49-54.
NEAL, L.S., and BANKOFF, S.G. (1965). "Local Parameters in Cocurrent Mercury-Nitrogen Flow." *Am. Inst. Chem. Jl*, Vol. 11, pp. 624-635.
PLUMPTRE, G. (1993). "The Water Garden." *Thames and Hudson*, London, UK.
RAJARATNAM, N., MAINALI, A., and HSUNG, C.Y. (1997). "Observations on Flow in Vertical Dropshafts in Urban Drainage Systems." *Jl of Envir. Eng.*, ASCE, Vol. 123, 486-491.
STRAUB, L.G., and ANDERSON, A.G. (1958). "Experiments on Self-Aerated Flow in Open Channels." *Jl of Hyd. Div.*, Proc. ASCE, Vol. 84, No. HY7, paper 1890, 35 pages.